CHAPTER 1

INTRODUCTION

1.1 Background of Study

Carbon dioxide (CO_2) corrosion is regarded as a major problem in oil & gas industry nowadays. Carbon dioxide systems are one of the most common environments in the oil field industry where corrosion occurs. Carbon dioxide forms a weak acid known as carbonic acid (H_2CO_3) in water, a relatively slow reaction. The presence of many other chemical species could or influence the kinetics of the corrosion.

In oil and gas industry, CO_2 corrosion has been a recognized problem in production and transportation facilities for many years. This result from the fact that an aqueous phase is normally associated with the oil and gas production systems which promote an electrochemical reaction between carbon steel and the contacting aqueous phase.

Most of the studies focused on general corrosion in CO_2 environment. However, most of the failures encountered in the field were of localized corrosion.

1.2 Problem Statements

Corrosion has become a major problem in most of platforms especially the pipelines which will lead to leakage and system failures eventually. A lot of researches have been done about CO_2 corrosion, but very few studies has been conducted about the Calcium ions (Ca^{2+}) effect on CO_2 corrosion, particularly on the possibility of pitting influence.

1.3 Objective of Study

The main objective of the project is to investigate the mechanism of Ca^{2+} ions in CO_2 corrosion leading to pitting corrosion using Electrochemical Impedance Spectroscopy (EIS).

1.4 Scope of Study

For this project, the scope of study includes conducting lab experiment to study the effect of calcium ions concentration on CO_2 corrosion using the method of Electrochemical Impedance Spectroscopy. The study includes measuring the corrosion rate of X52 carbon steel in 3 different environments, containing calcium and chloride ions.

CHAPTER 2

LITERATURE REVIEW

In oil and gas industry, CO_2 corrosion has been a recognized problem in production and transportation facilities for many years. It is a major source of concern in the application of carbon steel. This result from the fact that an aqueous phase is normally associated with the oil and gas production systems which promote an electrochemical reaction between carbon steel and the contacting aqueous phase. CO_2 is extremely soluble in water but has a greater solubility in hydrocarbon fluids produced in the oil and gas production systems and, although it does not cause the catastrophic failure mode of cracking associated with H_2S; its presence can nevertheless result in very high corrosion rate particularly where the mode of attack on carbon steel is localized.

In the oil and gas exploration/production, transportation, and processing industries, low-grade carbon steel represents the most commonly used construction material for pipelines. The resistance of materials to CO_2 corrosion is affected by the application of CO_2 gas injection for enhanced oil recovery and the active exploitation of deep natural gas reservoir containing CO_2 [1]. Depending upon the existing conditions, carbon steel corrosion may occur either as uniform or localized attack, the latter in the form of pitting corrosion, crevice corrosion, and stress corrosion cracking or corrosion fatigue. Pitting corrosion, rather than uniform corrosion, is the principal cause for failure of the producing and transporting equipment. In laboratory experiments, Schmitt and Rothman [2] found that pitting corrosion appeared for several non-alloyed and low-alloyed steels after prolonged exposure to oxygen-free CO_2-containing distilled water at 25°C. According to Schmitt [3], the highest susceptibility to pitting corrosion occurred at 60–80°C. In the sweet oil and gas fields, the formation water contained many other cations such as Ca^{2+}, Mg^{2+} and so on, which lead to precipitation of scale deposits and may influence the susceptibility to pitting corrosion and/or uniform corrosion. For example,

severe carbon dioxide corrosion of oil tubes was reported to occur in the Shengli oil Weld in Northern China where the stratum water is rich in calcium (15g/L) [4]. Although many studies in the laboratory [5,6] have been carried out to simulate CO_2 corrosion behavior of pipeline steel in NaCl solutions, less work has focused on corrosion problems of carbon steel in NaCl solution in the presence of Ca^{2+} [4,7] . Therefore in this project, it was decided to add Ca^{2+} (usually in the form of $CaCl_2$) into NaCl solution in the laboratory to simulate the aqueous medium from the real field in order to improve the understanding of carbon steel corrosion in the presence of Ca^{2+}. In the sweet oil and gas fields, the shutdown of pipeline happens for various reasons such as overhaul and causes corrosion in stagnant condition. After overhaul, when the pipelines and equipments run again, the corrosion behavior is somewhat different from that the pipelines and equipments experienced continually running. Under stagnant condition with high Fe supersaturation, corrosion product scale can easily form, which is believed to play an important role in the mechanism, kinetics, and pattern of CO_2 corrosion.

2.1 Basic Corrosion Theory

Corrosion is an electrochemical reaction composed of two half cell reactions, an anodic reaction and a cathodic reaction. The anodic reaction releases electrons, while the cathodic reaction consumes electrons. There are three common cathodic reactions, oxygen reduction (fast), hydrogen evolution from neutral water (slow), and hydrogen evolution from acid (fast).

2.1.1 The corrosion cell

Figure 2.1 shows the corrosion cell of a containing anode, cathode as well as

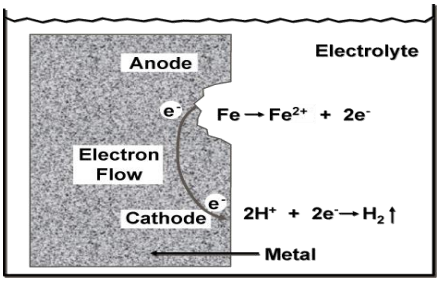

Figure 2.1 Basic Corrosion Cell

as the electron transfer from anode to cathode.

Anodic reaction:

$$M \rightarrow M^{n+} + ne^- \quad (2.1)$$

M stands for a metal and n stands for the number of electrons that an atom of the metal will easily release.

i.e. for iron and steel:

$$Fe \rightarrow Fe^{2+} + 2e^- \quad (2.2)$$

Cathodic reactions:

$$O_2 + 4\,H^+ + 4e^- \rightarrow 2H_2O \quad (2.3)$$

(oxygen reduction in acidic solution)

$$1/2\,O_2 + H_2O + 2e^- \rightarrow 2\,OH^- \quad (2.4)$$

(oxygen reduction in neutral or basic solution)

$$2\,H^+ + 2e^- \rightarrow H_2 \quad (2.5)$$

(hydrogen evolution from acidic solution)

$$2\,H_2O + 2e^- \rightarrow H_2 + 2\,OH^- \quad (2.6)$$

(hydrogen evolution from neutral water)

Each half-cell reaction has an electrical potential, known as the half-cell electrode potential. The anodic reaction potential, E_a , plus the cathodic reaction potential, E_c , adds up to E, the cell potential. If the overall cell potential is positive, the reaction will proceed spontaneously.

Every metal or alloy has a unique corrosion potential in a defined environment. When the reactants and products are at an arbitrarily defined standard state, the half-cell electrode potentials are designated E^o. These standard potentials are

measured with respect to the standard hydrogen electrode (SHE). A listing of standard half-cell electrode potentials is given in Table 1.

Selected half-cell reduction potentials are given in Table 1. To determine oxidation potentials, reverse the direction of the arrow and reverse the sign of the standard potential. For a given cathodic reaction, those anodic (reversed) reactions below it in the table will go spontaneously, while those above it will not. Thus any metal below the hydrogen evolution reaction will corrode (oxidize) in acidic solutions. For example,

Cathodic reaction:

$$2H^+ + 2e^- \rightarrow H_2 \qquad (2.7)$$

(hydrogen evolution)

Two possible anodic reactions:

$Cu \rightarrow Cu^{2+} + 2e^-$

(above cathodic reaction in table - will not corrode)

$$Zn \rightarrow Zn^{2+} + 2e^- \qquad (2.8)$$

(below cathodic reaction in table - spontaneous corrosion)

2.1.2 Why corrosion cells form

Corrosion cells are created on metal surfaces in contact with an electrolyte because of energy differences between the metal and the electrolyte. Different area on the metal surface could also have different potentials with respect to the electrolyte. These variations could be due to i) metallurgical factors, i.e., differences in their composition, microstructure, fabrication, and field installations, and ii) environmental factors. Carbon and low alloy steels are the most widely used material in the oilfield. Stainless steels (Fe-Cr-Ni), and nickel-base corrosion resistant alloys (CRA), such as Incoloys (Ni-Fe-Cr), Inconels (Ni-Cr), Hastelloys (Ni-Cr-Mo-Fe-Co) etc., are also used in highly corrosive environments.

i) *Metallurgical factors*

Steel is an alloy of iron (Fe) and carbon (C). Carbon is fairly soluble in liquid iron at steel making temperatures, however, it is practically insoluble in solid iron (0.02% at 723C), and trace at room temperature. Pure iron is soft and malleable; small amounts carbon and manganese are added to give steel its strength and toughness.

Most of the carbon is oxidized during steelmaking. The residual carbon and post-fabrication heat treatment determines the microstructure, therefore strength and hardness of steels. Carbon steels are then identified by their carbon contents, i.e., low-carbon or mild steel, medium carbon (0.2- 0.4 % C), high-carbon (up to 1% C) steels, and cast irons (>2 % C). American Iron and Steel Institute (AISI) designation 10xx series represent plain carbon steels, last two digits indicating the carbon content. For instance, AISI 1036 steel, commonly used in sucker rods, contain 0.36% carbon. Low alloy steels contain 1-3% alloying elements, such as chromium-molybdenum steels, 4140 (1% Cr-0.2% Mo-0.4% C), for improved strength and corrosion resistance. American Petroleum Institute (API) specifications also provide guidelines for strength and chemical composition of oilfield steels.

During equilibrium solidification of steel, individual grains of almost pure iron (ferrite), and grains richer in iron carbide (cementite, Fe_3C) within ferrite form. The lamellar carbide structure with ferrite is known as pearlite. If, however, steel is rapidly cooled to room temperature (quenched), carbon is retained in a highly strained matrix known as martensite. This structure is very hard and brittle and is not suitable for most engineering applications. The microstructure of fast cooled steels, for instance after welding or hot-rolling, are modified by reheating steels to a critical temperature range and controlled cooling, i.e., tempering, normalizing, and annealing.

ii) Environmental factors

Sections of the same steel may corrode differently due to variations in the concentration of aggressive ions in the environment. For instance, a casing or a pipeline could pass through several formations or soils with different water composition, hence, sections of the casing or the pipe could experience different rates of corrosion. Similarly, a pipeline crossing a river will be exposed to higher concentration salts as compared to dry land. It is difficult to predict the effect of higher salt concentrations but, generally, sections of steel exposed to higher salt concentrations become anodic and corrode.

Differences in the oxygen concentration on the metal surface (differential aeration or differential oxygen concentration cells) cause particularly insidious forms of corrosion. A common example is corrosion of pipes under paved roads, parking lots, or pavements.

Lack of oxygen under the pavement render that section of the pipe anodic, hence pipe corrodes preferentially. Similarly, loose backfill placed into ditch to cover a pipeline is more permeable to oxygen diffusion; the topside of the pipe will become cathodic, and the bottom resting on undisturbed soil will become anodic and corrode. Crevice and pitting corrosion mechanisms in aerated systems can also be explained by differential concentration cells.

2.2 Overview of Carbon Dioxide Corrosion

2.2.1 Carbon Dioxide (CO_2) Gas

Carbon dioxide systems are one of the most common environments in the oil field industry where corrosion occurs. Carbon dioxide forms a weak acid known as carbonic acid (H_2CO_3) in water, a relatively slow reaction. However, CO_2 corrosion rates are greater than the effect of carbonic acid alone. Cathodic depolarization may occur, and other attack mechanisms may also be at work. The presence of salts is relatively unimportant.

Corrosion rates in a CO_2 system can reach very high levels (thousands of mils per year), but it can be effectively inhibited. Velocity effects are very important in the CO_2 system; turbulence is often a critical factor in pushing a sweet system into a corrosive regime. This is because it either prevents formation or removes a protective iron carbonate (siderite) scale.

Conditions favoring the formation of the protective iron carbonate scale are elevated temperature, increased pH (bicarbonate waters) and lack of turbulence. Magnetite scales are also formed in CO_2 systems, and corrosion product scales often consist of layers or mixtures of siderite and magnetite.

The maximum concentration of dissolved CO_2 in water is 800 ppm. When CO_2 is present, the most common forms of corrosion include uniform corrosion, pitting corrosion, wormhole attack, galvanic ringworm corrosion, heat affected corrosion, mesa attack, raindrop corrosion, erosion corrosion, and corrosion fatigue. The presence of carbon dioxide usually means no H_2 embrittlement.

CO_2 corrosion products include iron carbonate (siderite, $FeCO_3$), Iron oxide, and magnetite. Corrosion product colors may be green, tan, or brown to black. CO_2 corrosion is one of the most common environments where corrosion occurs, and exists almost everywhere.

Areas where CO_2 corrosion is most common include flowing wells, gas condensate wells, areas where water condenses, tanks filled with CO_2, saturated produced water and flowlines, which are generally corroded at a slower rate because of lower temperatures and pressures. CO_2 corrosion is enhanced in the presence of both oxygen and organic acids, which can act to dissolve iron carbonate scale and prevent further scaling.

Prediction of corrosion

In sweet gas wells with a pH of 7 or less,

a CO_2 partial pressure of 30 psi usually indicates corrosion.
a CO_2 partial pressure of 7 - 30 psi may indicate corrosion.
a CO_2 partial pressure of 7 psi is usually considered non-corrosive.

2.2.2 Mechanism of Carbon Dioxide Corrosion

Dry CO_2 gas by itself is not corrosive at the temperatures encountered within oil and gas production systems. It becomes corrosive when dissolved in an aqueous phase through which it can promote an electrochemical reaction between steel and the contacting aqueous phase. Various mechanisms have been postulated for the CO_2 corrosion process but all involve either carbonic acid (H_2CO_3) or the bicarbonate ion ($2HCO_3^-$) formed on dissolution of CO_2 in water. The step for the CO_2 corrosion process is presented by the reaction shown in the equations as follows:

$$CO_{2\,(aqueous)} + H_2O \leftrightarrow H_2CO_3 \leftrightarrow H^+ + HCO_3^- \quad (2.9)$$

The mechanism suggested by de Waard is:

$$H_2CO_3 + e^- \rightarrow H + HCO_3^- \quad (2.10)$$

$$2H \rightarrow H_2 \quad (2.11)$$

With the steel reacting:

$$Fe \rightarrow Fe^{2+} + 2e^- \quad (2.12)$$

The overall equation is:

$$CO_2 + H_2O + Fe \rightarrow FeCO_3 + H_2 \quad (2.13)$$

Besides, CO_2 corrosion also results from the practice of pumping CO_2 saturated water into wells to enhance oil recovery and reduce the viscosity of the pumped fluid. The presence of CO_2 in solution leads to the formation of a weak carbonic acid which drives CO_2 corrosion reactions [8]. The initiating process is presented by the reaction shown in equation (2.14).

$$CO_2 + H_2O \leftrightarrow H_2CO_3 \quad (2.14)$$

The following corrosion process is controlled by three cathodic reactions and one anodic reaction. The cathodic reactions, include (2.15a) the reduction of carbonic acid into bicarbonate ions, (2.15b) the reduction of bicarbonate ions, and (2.15c) the reduction of hydrogen ions:

$$2H_2CO_3 + 2e^- \rightarrow H_2 + 2HCO_3^- \quad (2.15a)$$

$$2HCO_3^- + 2e^- \rightarrow H_2 + 2CO_3^{2-} \quad (2.15b)$$

$$2H^+ + 2e^- \rightarrow H_2 \quad (2.15c)$$

The anodic reaction significant in CO_2 corrosion is the oxidation of iron to ferrous (Fe^{2+}) ion given in equation (2.16).

$$Fe \rightarrow Fe^{2+} + 2e^- \quad (2.16)$$

These corrosion reactions promote the formation of $FeCO_3$ which can form along a couple of reaction paths. First, it may form when ferrous ions react directly with carbonate ions as shown in equation (2.17). However, it can also form by the two processes shown in equations (2.18a, 2.18b). When ferrous ions react with bicarbonate ions, ferrous iron bicarbonate forms which subsequently dissociates into iron carbonate along with carbon dioxide and water.

$$Fe^{2+} + CO_3^{2-} \rightarrow FeCO_3 \quad (2.17)$$

$$Fe^{2+} + 2HCO_3^- \rightarrow Fe(HCO_3)_2 \quad (2.18a)$$

$$Fe(HCO_3)_2 \rightarrow FeCO_3 + CO_2 + H_2O \quad (2.18b)$$

The significance of $FeCO_3$ formation is that it drops out of solution as a precipitate due to its limited solubility. This precipitate has the potential to form passive films on the surfaces of carbon steel which may reduce their corrosion.

2.3 Electrochemical Measurement Techniques

It is important to measure and predict CO_2 corrosion rate as it would determine the materials to be used for production and transportation facilities, in the oil and gas industry. In this project, the effect of $CaCO_3$ and $FeCO_3$ deposit formation on CO_2 corrosion rate will be analyzed using EIS and all the data obtained from the experiments would assist in providing a reliable prediction on the behavior of CO_2 corrosion that will leads to cost-effective and safe design of production and transportation facilities used in the oil and gas industry. The sample was taken from the oil and gas industrial transportation pipelines using X52 mild steel.

2.3.1 Electrochemical Impedance Spectroscopy (EIS)

EIS is one of the electrochemical methods to measure corrosion rate. In recent years EIS has been used to study corrosion mechanisms intensively. EIS can be an alternative method when corrosion methods using Tafel methods cannot be used. Electrochemical impedance measures corrosion rate by applying an AC potential to an electrochemical cell and measuring the current through the cell without significantly disturbing the properties of the surface [9]. EIS technique uses a small excitation signal ranging 5 to 50 mV and in the range of frequencies of 0.001 Hz to 100,000 Hz. Moreover, EIS presents a qualitative and quantitative analyses of surface characteristics. EIS also can give information about process occurring on the metal surface during corrosion and further provides corrosion

mechanisms on the surface. For those reasons, EIS usually used to evaluate corrosion inhibitor behavior, anodic coating and other surface formation process.

The EIS instrument records the real (Z`) and imaginary (Z``) components of the impedance response of the system. The real part is plotted on the X axis and the imaginary part on the Y axis of a chart, so called as Nyquist plot. EIS also can be used to study surface properties by using correlation of impedance (Z) and phase angle as drawn at the figure below.

The impedance is then represented as a complex number,

$$Z(j\omega) = Z'(\omega) + jZ''(\omega)$$

The magnitude of impedance is:

$$|Z| = \sqrt{|Z'|^2 + |Z''|^2} \qquad (2.19)$$

$$\mathrm{Re}(Z) = |Z|\cos\phi$$

$$\mathrm{Im}(Z) = |Z|\sin\phi$$

Where:

Z` is real axis

Z`` is imaginary axis

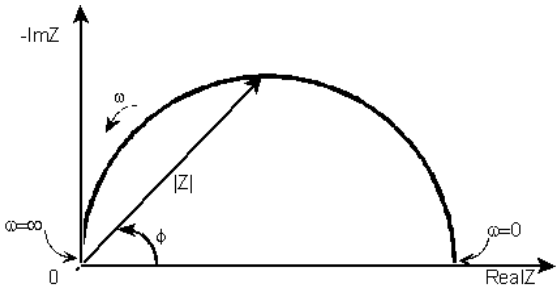

Figure 2.2: Relationship between the magnitude of impedance (Z) and phase angle

As can be seen, during corrosion reaction, it will be several possibilities occurring on the metal surface. There are activation reaction and mass transfer. The activation reaction is process which is controlled by charge transfer reaction. While, mass transfer reaction is driven by diffusion process as an effect of double layer behavior. EIS presents such two mechanisms as shown in figure 2.3, 2.4 and 2.5. Figures 2.3 below present the activation reaction mechanisms that might happen on the surface during corrosion reaction as plotted on the Nyquist plot. Next, Figure 2.4 represents the mass transfer of the reaction while Figure 2.5 represents the combination of the 2 process reactions.

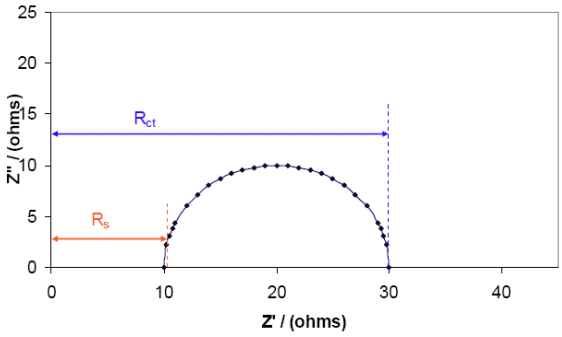

Figure 2.3: Shape of Nyquist plot in corrosion controlled by charge transfer reaction

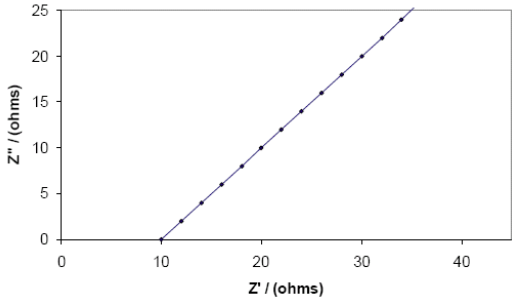

Figure 2.4: Shape of Nyquist plot in corrosion controlled by charge transfer reaction

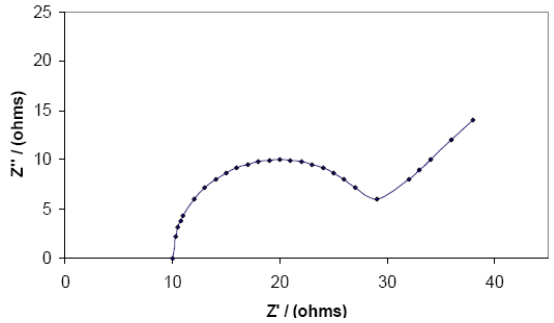

Figure 2.5: Shape of Nyquist plot in corrosion controlled by combination reaction process (charge transfer and mass transfer)

Equivalent circuit models

Further interpretation can be conducted using an assumption of equivalent electrical circuit consists of resistor and capacitor arrangements [10]. These elements can be combined in series and parallel to simulate cell corrosion in the system. Through this circuit, properties of the surface can be identified as a circuit analogue. It includes a solution resistance, a double layer capacitor and a charge transfer or polarization resistance. The simple equivalent circuit is presented in the figure 2.6 and Figure 2.7 below.

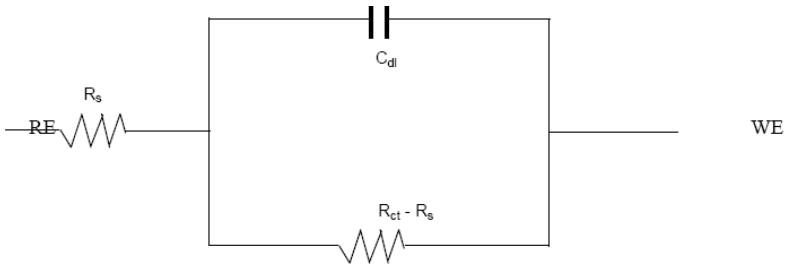

Figure 2.6: Equivalent circuit for cell experiment in activation process reaction

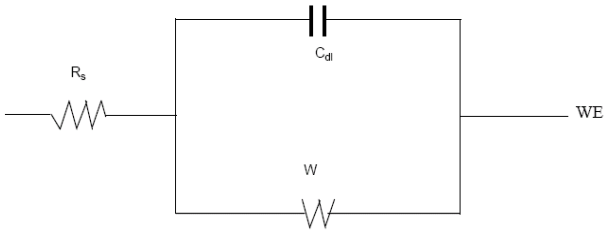

Figure 2.7: Equivalent circuit for cell experiment in diffusion process reaction

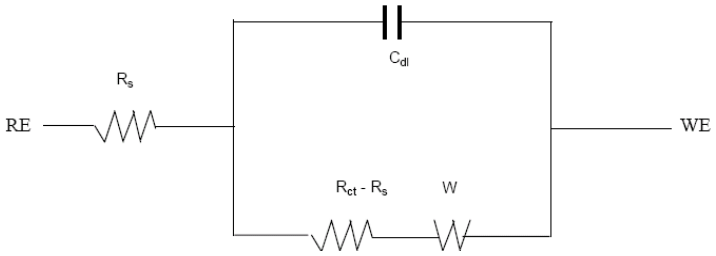

Figure 2.8: Equivalent circuit for cell experiment in by combination reaction process (charge transfer and mass transfer)

Double Layer Capacitance

Corrosion reaction occurring on the electrode/solution interface can produce an electrical double layer. This double layer is formed as barrier ions from the solution and the electrode surface [11]. Those double layer charges are separated by insulator similar to the capacitor. The separation is very small, on the order of angstroms. The value of the double layer capacitance depends on many variables including electrode potential, temperature, ionic concentrations, types of ions, oxide layers, electrode roughness, impurity adsorption.

Diffusion process

Corrosion mechanism on the metal surface can also be controlled by diffusion process. If electron flows through the film, these AC signal will penetrate to the surface creating an impedance known as the Warburg impedance. This impedance depends on the frequency of the potential perturbation. At high

frequencies the Warburg impedance is small since diffusing reactants do not have to move very far. At low frequencies the reactants have to diffuse farther, thereby increasing the Warburg impedance. The value of the Warburg impedance can be infinite. The equation for the infinite Warburg impedance is:

$$Z = \sigma(\omega)^{-1/2}(1 - j) \tag{2.20}$$

On a Nyquist plot the infinite Warburg impedance appears as a diagonal line with a slope of 0.5. On a Bode plot, the Warburg impedance shows a phase shift of 45°.

In equation 2-21, s is the Warburg coefficient defined as:

$$\sigma = \frac{RT}{n^2 F^2 A\sqrt{2}}\left(\frac{1}{C_O^*\sqrt{D_O}} + \frac{1}{C_R^*\sqrt{D_R}}\right) \tag{2.21}$$

In which,

w = radial frequency

D_O = diffusion coefficient of the oxidant

D_R = diffusion coefficient of the reductant

A = surface area of the electrode

n = number of electrons transferred

C* = bulk concentration of the diffusing species (moles/cm^3)

This form of the Warburg impedance is only valid if the diffusion layer has an infinite thickness. Quite often this is not the case. If the diffusion layer is bounded, the impedance at lower frequencies no longer obeys the equation above. Instead, we get the form:

$$Z_O = \sigma\omega^{-1/2}(1 - j)\tanh\left(\delta\left(\frac{j\omega}{D}\right)^{1/2}\right) \tag{2.22}$$

with,

d = Nernst diffusion layer thickness

D = an average value of the diffusion coefficients of the diffusing species

This more general equation is called the "finite" Warburg. Equation 2-22 simplifies to the infinite Warburg impedance. Warburg impedance was developed to model this phenomenon. Several expressions, based on different assumptions, are used to describe diffusion impedance.

CHAPTER 3
METHODOLOGY

3.1 Research Methodology

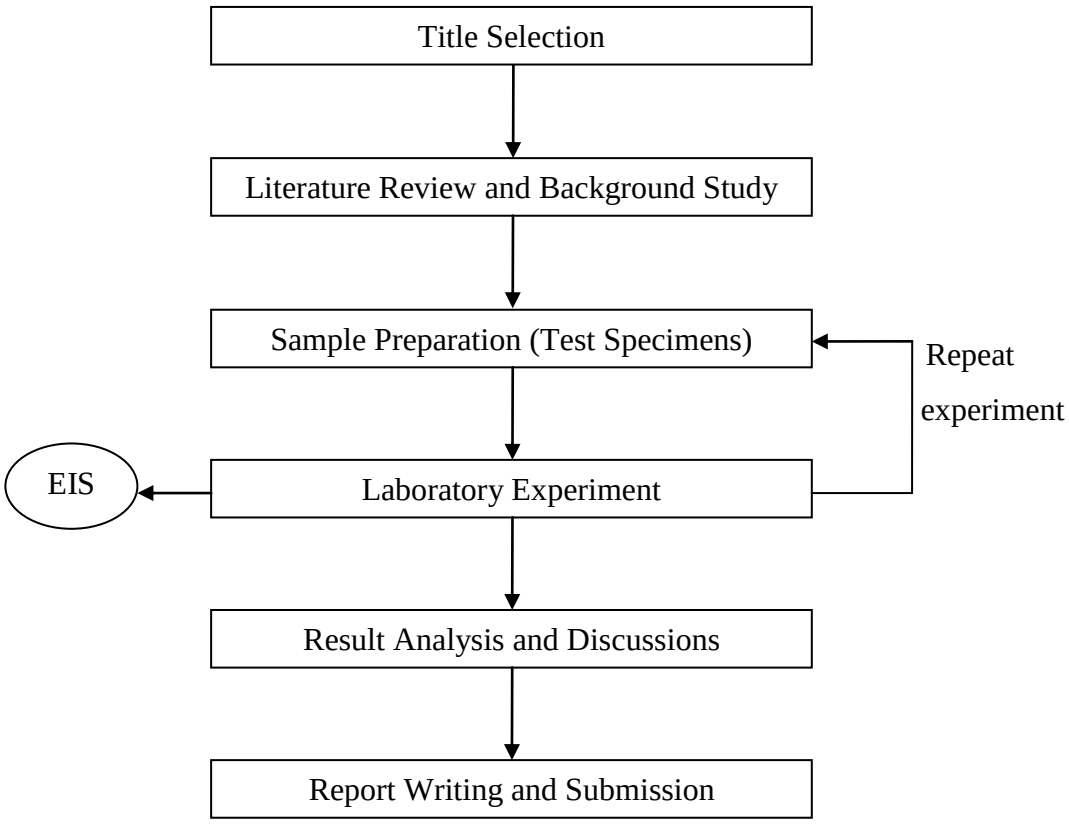

Figure 3.1: Project flow chart

From Figure 3.1, it shows the project flow chart where research were done on some resources such as books, journals and technical papers specifically on CO_2 corrosion of carbon steel, effects of adding calcium in oxygen-free CO_2-containing solution environment and EIS technique. Besides, consultation sessions with the supervisor and related personnel were also held in order to get a better understanding on the EIS technique. The laboratory experiments were conducted on X52 mild steel in stagnant

condition using 3% wt NaCl, 4.6 % wt NaCl and 3.0 % wt NaCl + 1.5 % wt NaCl to study the effect of the calcium ions on the corrosion rate. EIS technique was employed to study and analyze CO_2 corrosion rate and formation of protective $FeCO_3$ film layers. In this case, LPR is also used for comparison. Once the results were obtained, analysis was done using SEM technique. Lastly, final report was written to complete this project.

3.2 Electrochemical Measurement Techniques

3.2.1 Electrochemical Impedance Spectroscopy (EIS)

The fundamental approach of EIS technique is to apply a small amplitude sinusoidal excitation signal usually a voltage between 5 to 10 mV which is applied to the working electrode over a range of frequencies, ω of 0.001 Hz to 100,000 Hz. The usual result is a Nyquist plot of half a semi-circle, the high frequency part giving the solution resistance and the width of the semi-circle. The analysis of this data is performed by circle fitting in the analysis software. One useful benefit of EIS technique is the ability to measure the solution resistance at high frequency.

3.3 Materials

The working electrode was made from X 52 low carbon steel. The sample was taken from the transportation pipelines used in oil and gas industry.

3.4 Sample Preparation

3.4.1 Cutting and Turning Process

1) Piece of transportation pipe of X52 carbon steel is transported from site to UTP.

2) The pipe is sliced into smaller parts using motor driven belt chain saw to make it easier of fabricating it into test specimens' size.

3) From the small pieces of 15cm thickness, turning process using conventional lathe machine is used to fabricate the work piece test specimens' measuring 1cm in diameter.

4) The work piece test specimens are then sliced into few small pieces in order to be prepared for the next procedure of sample preparation.

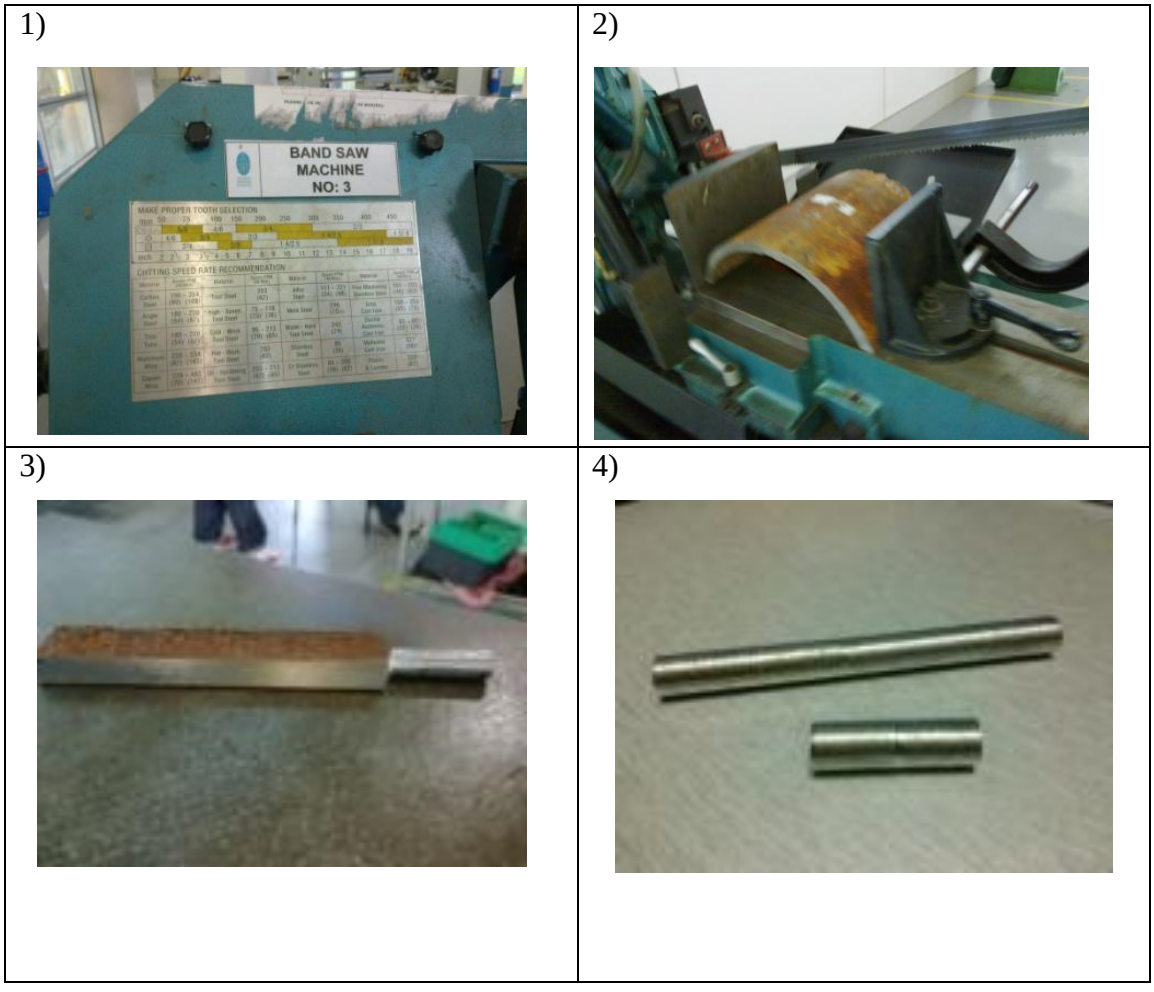

Figure 3.2: Sequence of preparing test specimens in cutting and turning process

3.4.2 Cold Mounting and Metallurgical Grinding

Then, the test specimens were mounted with epoxy by cold mounting as shown in Figure 3.3 and grinded with wet silicon carbide (SiC) paper with a final wet grind using 120, 320, 600 and 1200 grit SiC paper shown in Figure 3.4. Finally, the test specimens were rinsed with deionizer water and degreased with acetone prior to immersion.

Figure 3.3: Specimens being Cold -Mounted

Figure 3.4: Grinding Process

3.5 Experimental Setup

3.5.1 Test Matrix

Table 3.1 shows the test matrix for studying corrosion on the coupon with the presence of carbon dioxide gas only (purging CO_2 gas only to eliminate the presence of oxygen in solution which is called de-oxygenation process).

Table 3.1: Corrosion rate investigation for varying content of Ca^{2+} ions in the experiment

Parameters	Details
Solutions	3.0% NaCl, 4.6% NaCl, 3.0% NaCl + 1.5% $CaCl_2$,
Experiment temperature(^oC)	25(room temperature)
Duration of experiment (hours)	24 hours (reading every 1 hour)
Purging duration	1 hour supply of CO_2 (deoxygenation)
Coupon presence	Yes
Types of coupon	Carbon steel X52 (Used for transportation pipe)
pH	4.7
Chemical assays	Sodium chloride, Calcium chloride
Presence of ions	Ca^{2+}, Cl^-, Na^+

3.5.2 Experiment Procedure

1) 1 liter of sodium chloride solution is prepared in a beaker.
2) The solution is set up at room temperature. Stirrer is placed inside the solution to ensure the solution become aqueous.
3) $NaHCO_3$ is added to the solution in order to maintain the pH of solution. The ideal pH should be around 4.7.
4) The equipments are set up as in Figure 3.3. Each working electrode 1 & 2, reference electrode and auxiliary electrode is connected to the respective wire from AutoLab machine.

5) For EIS, both test specimens are connected to the labeled wire electrode 1 and 2 from ACM / AutoLab machine to measure the corrosion rate.
6) Auxiliary and reference electrodes immersed in the solution are connected respectively to each slot on the ACM machine. The overall setup can be shown in Figure 3.5
7) The ACM machine shown in Figure 3.6 is setup to record the corrosion rate data for the mild steel specimens. Readings are taken every 15 minutes and the experiment is conducted for a 1 day period before data can start to be collected.
8) Repeat step 1-8 using different amount of sodium chloride and calcium chloride according to the desired weight percentage.

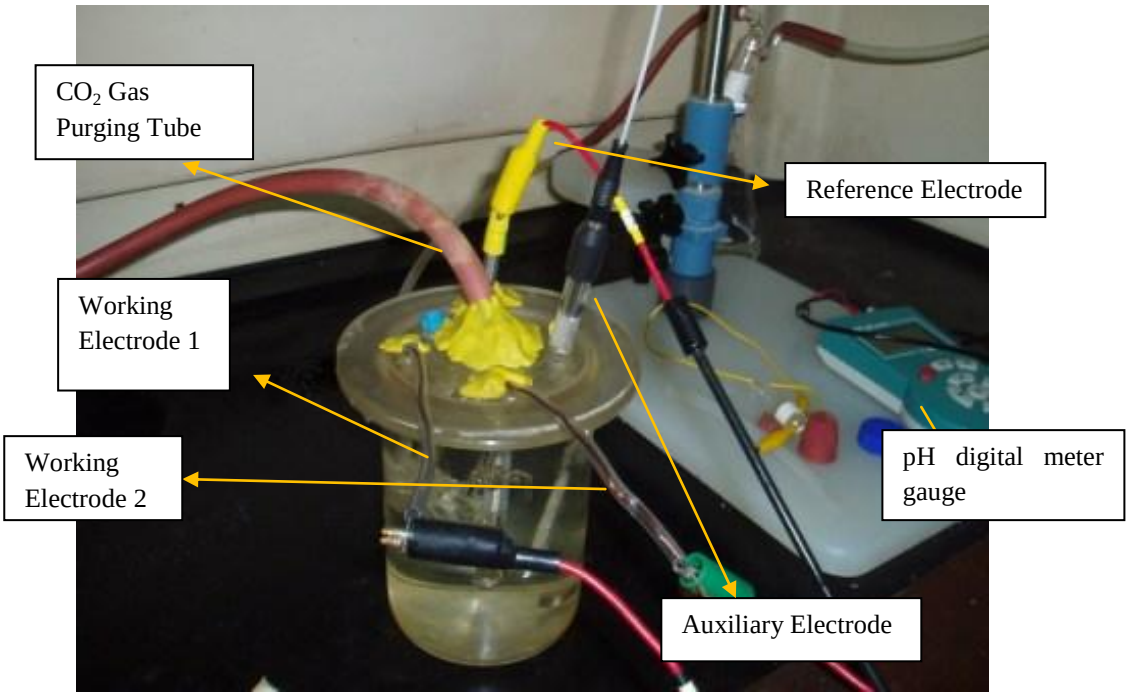

Fig 3.5: Setup of the experiment

Figure 3.6: ACM Instrument machine used to measure corrosion rate using EIS

CHAPTER 4
RESULTS AND DISCUSSION

4.1 Effect of Calcium Ions on CO_2 Corrosion

The results of the experiment conducted in CO_2 corrosion environment are presented in this chapter. In this chapter the effect of calcium ion as well as chloride ions on CO_2 corrosion is considered. Firstly, the concentration of NaCl which represented the salinity and the environment of underwater saltwater were taken as the reference point. Next by adding specified amount of calcium ions (Ca^{2+}) in the form of calcium chloride, $CaCl_2$, the effect of calcium is being investigated. By adding $CaCl_2$ in the second experiment, it means that we are adding more concentration of Cl^- ions. The result can be due to the effect of adding calcium or chloride ions. Therefore, a third experiment is carried out by investigating the effect of chloride ion by the same concentrations of chloride ions as in the second experiment.

4.1.1 Corrosion Rate of X52 carbon steel in three different environments

Table 4.1 showed the corrosion rate data of X52 carbon steel immersed in three different environments for 24 hours to investigate the effect of Ca^{2+} ions on CO_2 corrosion. Figure 4.1 shows the corrosion rate of X52 carbon steel test specimen immersed in 3 different environments for 24 hours. From the result, it clearly shown that corrosion rate is highest in 4.6% NaCl solution followed by 3% NaCl + 1.5% $CaCl_2$ and the lowest in 3% NaCl solution. All solutions are saturated with CO_2 gas and tested at room temperature of 25^oC.

Table 4.1: Corrosion Rate recorded by EIS in three different environments

	Corrosion Rate (mm/yr)		
Time	3% NaCl	3% NaCl + 1.5% CaCl2	4.6% NaCl
1	0.45	0.62	1.64
4	0.24	0.33	1.24
8	0.17	0.23	1.19
12	0.12	0.22	1.39
16	0.1	0.2	1.19
20	0.09	0.19	1.23
24	0.09	0.21	1.23

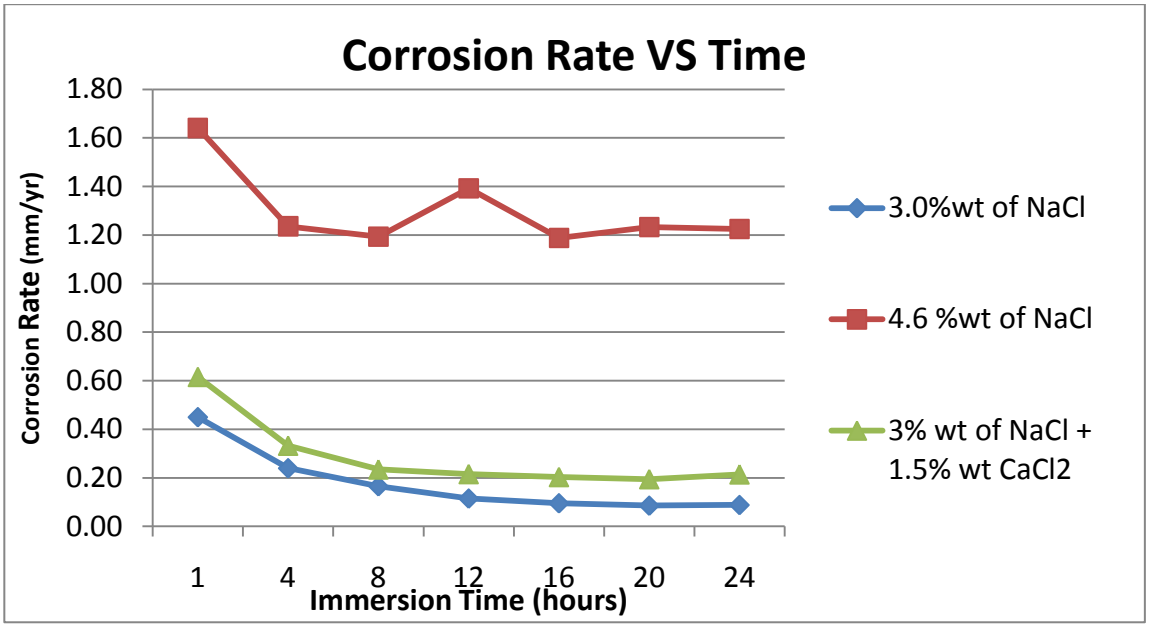

Figure 4.2: Corrosion Rate vs. time graph of X52 carbon steel immersed in three different environments for 24hours

From Table 4.1, the average corrosion rate is calculated and the result is shown in Table 4.2. The result showed that with increasing Cl^- concentration, the corrosion rate increased. This is proven by the value of corrosion rate in 4.6% NaCl, at 1.30 mm/yr. which is higher compared to 3% NaCl which is 0.18 mm/yr However, at the same concentration of Cl^-, the addition of calcium ions

decreased the corrosion rate, at 0.29 mm/yr. By adding Ca^{2+} ions by 1.5%, the corrosion rate decreased by 1.01 mm/yr. This shows that Ca^{2+} influenced the corrosion rate of the test specimen in CO_2 corrosion.

Table 4.1: Average Corrosion Rate taken by EIS in 3 different environments

Solution	Average Corrosion Rate(mm/yr)
3% NaCl	0.18
4.6% NaCl	1.30
3.0% NaCl + 1.5% CaCl2	0.29

4.1.2 Corrosion Rate of X52 carbon steel in 3% NaCl, CO_2 saturated at 25°C

Figure 4.2 shows Nyquist plot X52 carbon steel in 3% NaCl saturated by CO_2 under stagnant condition.

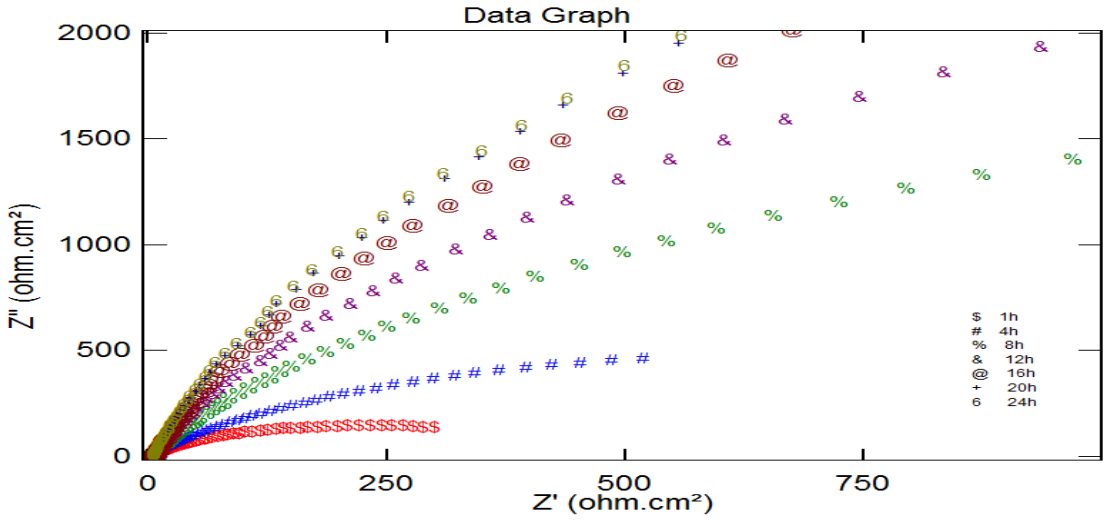

Figure 4.3: Nyquist plot of X52 carbon steel immersed in 3% NaCl, CO_2 saturated environment, 25°C, natural pH

From the Nyquist plot, the corrosion rate decreased with from immersion time 1hour until 24 hours. The diameters of the Nyquist plot increased from 1hour until 24hours, showing that corrosion rate decreased. The corrosion rate data of X52 carbon steel for this environment is shown in Table 4.3.

Table 4.3: Corrosion Rate of X52 carbon steel in 3% NaCl, CO2 saturated at 25^{o}C

Time (hour)	Corrosion Rate(mm/yr)
1	0.45
4	0.24
8	0.17
12	0.12
16	0.1
20	0.09
24	0.09
Average CR	**0.18**

The corrosion rate decreased from 0.45 mm/yr at 1h until 0.09 mm/yr at immersion time of 24 hours. As compared to other environment, the average corrosion rate is the lowest which is 0.18 mm/yr since it has the lowest concentration of Cl^- ions.

4.1.3 Corrosion Rate of X52 carbon steel in 3% NaCl + 1.5% $CaCl_2$, CO_2 saturated at 25^{o}C

Nyquist plot for X52 carbon steel immersed in 3% NaCl + 1.5% $CaCl_2$, saturated CO_2 solution at 25^{o}C is shown in Figure 4.2.

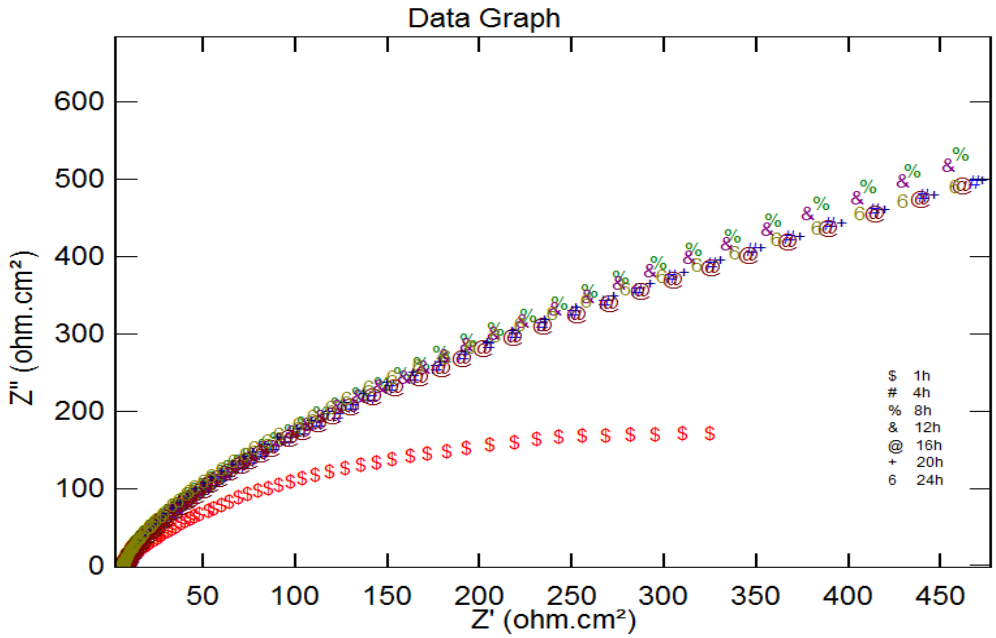

Figure 4.4: Nyquist plot of X52 carbon steel immersed in 3% NaCl + 1.5% $CaCl_2$, CO_2 saturated environment, 25^{o}C, natural pH

The diameters of the Nyquist plot increased from immersion time 1 hour until 24 hours. This showed that the corrosion rate of the specimen decreased from immersion time of 1hour until 24hours. Table 4.4 showed the corrosion rate for the specimen immersed in this environment.

Table 4.4 Corrosion rate of X52 carbon steel in 3% NaCl + 1.5% $CaCl_2$, CO_2 saturated at 25^{o}C.

Time (hour)	Corrosion Rate(mm/yr)
1	0.62
4	0.33
8	0.23
12	0.22
16	0.2
20	0.19
24	0.21
Average CR	**0.29**

The corrosion rate for the specimen in this environment decreased from immersion time of 1 hour until 24 hours. The corrosion rate at 1h is 0.62 mm/yr, decreased to 0.21 mm/yr at the end of the experiment (24hours). The average corrosion rate is 0.29 mm/yr, which is higher than corrosion rate of specimen immersed in 3% NaCl, CO_2 saturated solution which is 0.18 mm/yr. This is due to higher concentration of chloride ions in this environment, causing the corrosion rate to be higher.

4.1.4 Corrosion Rate of metal in 4.6% NaCl, CO_2 saturated at 25°C

For comparison purpose, a same experiment as the previous two but using 4.6% NaCl was carried out in order to verify whether Ca^{2+} ions could influence CO_2 corrosion. Nyquist plot for metal in 4.6% NaCl, CO_2 saturated at 25°C is shown in Figure 4.3.

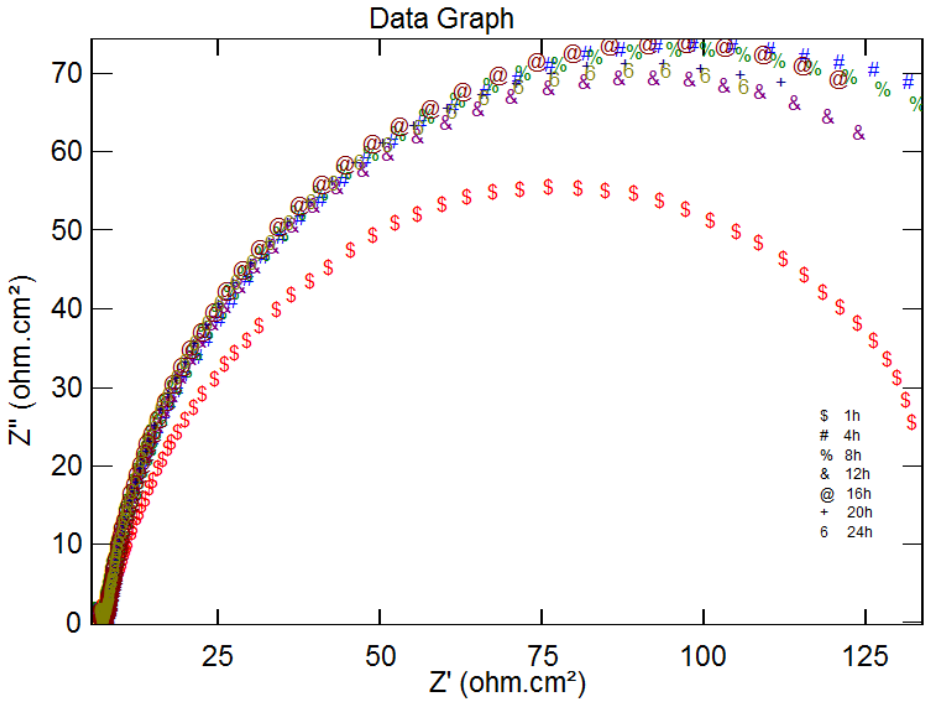

Figure 5.4: Nyquist plot for X52 carbon steel immersed in 4.6% NaCl, CO_2 saturated solution, 25°C natural pH

From the Nyquist plot in Figure 4.4, the diameters of the semicircles increased trend as the immersion time increased. This result showed that the corrosion rate decreased as the immersion time increased from 1 hour to 24 hours. The corrosion rate data for X52 carbon steel immersed in this environment is shown in Table 4.5

Table 2.5 Corrosion Rate of X52 carbon steel in 4.6% NaCl, CO_2 saturated at 25^{o}C.

Time (hour)	Corrosion Rate(mm/yr)
1	1.64
4	1.24
8	1.19
12	1.39
16	1.19
20	1.23
24	1.23
Average CR	**1.30**

The corrosion rate for X52 carbon steel immersed in this environment decreased from 1.64 mm/yr to 1.19 mm/yr at immersion time of 1 hour to 20 hours, but increased again until 24 hours. The average corrosion rate measured is 1.30 mm/yr, which is the highest compared to 3% NaCl and 3% NaCl + 1.5 $CaCl_2$ environments.

4.2 Discussion on the Calcium Ions (Ca^{2+}) Effect on CO_2 Corrosion

From the results obtained, the highest corrosion rate for X52 carbon steel is recorded in 4.6% NaCl, CO_2 saturated at 25^{o}C, followed by 3% NaCl + 1.5 $CaCl_2$ and the lowest corrosion rate is in 3% NaCl. The average corrosion rates measured are 1.30 mm/yr, 0.29 mm/yr and 0.18 mm/yr respectively. Increasing the concentration of Cl^- ions will result in higher corrosion rate, but with the presence of Ca^{2+} ions, the corrosion rate is reduced from 1.30 mm/yr to 0.29 mm/yr.

The result showed that Ca^{2+} ions could influence CO_2 corrosion, as the corrosion rate decreased by comparing 2 different environments having the same concentration of Cl^- ions. Ca^{2+} ions decreased the corrosion rate of the X52 carbon steel specimen due to scaling. Corrosion product solids form directly from the corroding metal.

CHAPTER 5
CONCLUSION AND RECOMMENDATION

5.1 Conclusion

Under stagnant condition, the corrosion rate in the blank solution increased with the increase of Cl^- concentration from 3% NaCl solution to 4.6% NaCl solution. For the solutions with the same Cl^- concentration, 3% NaCl + 1.5% $CaCl_2$ the corrosion rate decreased due to the addition of Ca^{2+}.

EIS can be used to measure the corrosion rate of X52 carbon steel specimens precisely, by studying the curve of the result obtained.

5.2 Recommendations

Throughout the entire project carried out during the final semester, the following recommendations can be implemented to improve the result of the project:

i. SEM analysis is required to verify the existence of coating layer by $CaCO_3$ and the pitting form on the metal surface. In this situation the formation of pitting corrosion can be observed physically.
ii. More lab work required for verifying the result - this can be conducted by running using another approach such as EIS and LPR.
iii. The studies need to be expanded to other elements such as Mg^{2+}:in real environment situation, Ca^{2+} is not the only type of ions exist in the environment.

REFERENCES

[1] Ikeda, M. Ueda, S. Mukai, Corrosion/85, paper No. 29, NACE, Houston, TX, 1985.

[2] G. Schmitt and B. Rothmann, *Werkstoffe und Korrosion* **29** (1978), p. 167.

[3] G. Schmitt, *Advances in CO_2 Corrosion* **1**, NACE, Houston, TX (1985) p. 1.

[4] S.L. Wu, Z.D. Cui, G.X. Zhao, M.L. Yan, S.L. Zhu and X.J. Yang, Applied Surface Science **228** (2004) (1–4), p. 17.

[5] X.Y. Zhang, F.P. Wang, Y.F. He, Y.L. Du, Corrosion Science 43 (2001) 1417.

[6] C.A. Palacios, J.R. Shadley, Corrosion 47 (2) (1991) 122.

[7] Z. Xia, K.-C. Chou, Z. Szklarska-Smialowska, Corrosion 45 (8) (1989) 636.

[8] Kewei Gao *, Fang Yu, Xiaolu Pang, Guoan Zhang, Lijie Qiao, Wuyang Chu, Minxu Lu *Mechanical properties of CO2 corrosion product scales and their relationship to corrosion rates* Volume 50, Issue 10, October 2008, Pages 2796-2803

[9] E. Yeager, J.O'M. Bockris, B.E. Conway, S. Sarangapani, Chapter 4 "AC Techniques *Comprehensive Treatise of Electrochemistry; Volume 9 Electrodics: Experimental Techniques*; ", M. Sluyters-Rehbach, J.H. Sluyters, Plenum Press, 1984.

[10] Fletcher, S., "Tables of Degenerate Electrical Networks for Use in the Equivalent-Circuit Analysis of Electrochemical Systems", *J. Electrochem. Soc.*, **141** (1994) 1823.

[11] Mansfeld, F., "Electrohemical Impedance Spectroscopy (EIS) as a New Tool for Investigation Methods of Corrosion Protection", *Electrochimica Acta*, **35** (1990), 1533

APPENDICES

Appendix I: EIS data taken for result for the experiment

Appendix II: Fyp II Ghantt Chart

No	Activities/ work		2	3	4	5	6	7	8	9	10	12	13	14
1	**Gathering all apparatus, fabrication process of metal piece test specimen and experiments equipment**													
2	**Research and Literature Review**													
3	**Setting up experiments, meetings with Graduate Assistants(GA)**													
4	**Experimental Work on to measure corrosion rate of CO_2 corrosion of test specimens**													
5	**Experimental Work on to measure corrosion rate (CO_2 corrosion) of test specimens with effect of calcium ions**													
6	**Submission of Progress Report 1**													
7	**Submission of Progress Report 2**													
8	**Seminar**													
9	**Poster Exhibition**													
10	**Submission of Dissertation Final Draft**													
11	**Oral Presentations**	**During Study Week**												
12	**Submission of Dissertation (Hard Bound)**	**7 days after oral presentation**												